J. Chem. Sci., Vol. 118, No. 6, November 2006, pp. 475–486.

Utilization of LVO_2^- species (L^{2-} is a tridentate ONS donor) as an inorganic analogue of carboxylate group: A journey to a new domain of coordination chemistry

SATYABRATA SAMANTA[a], SUBODH KANTI DUTTA[a,b] and MUKTIMOY CHAUDHURY[a,*]

[a]Department of Inorganic Chemistry, Indian Association for the Cultivation of Science, Kolkata 700 032
[b]Present address: Department of Chemistry, Western Michigan University, Kalamazoo, MI 49008, USA
e-mail: icmc@iacs.res.in

Abstract. The anionic *cis*-dioxovanadium (V) complex species LVO_2^- of tridentate biprotic dithiocarbazate-based ligands H_2L (*S*-methyl-3-((5-R-2-hydroxyphenyl)methyl)dithiocabazate, R = H, L = L^1; and R = Br, L = L^2) can bind alkali metal ions. The products $[LVO_2M(H_2O)_n]$ (M = Na^+, L = L^1, **1**; L = L^2, **2** and M = K^+, L = L^1, **3**) have extended chain structures in the solid state, stabilized by strong hydrogen bonding and Coulombic interactions as revealed from X-ray crystallography. The LVO_2^- moieties here behave like analogues of carboxylate groups and display interesting variations in their binding patterns. It appears that **1** is a single stranded helicate with LVO_2^- units forming the strands which surround the labile sodium ions occupying positions on the axis. The compounds are stable in water and methanol as solvents, while in aprotic solvents of higher donor strengths, viz. CH_3CN, DMF and DMSO, they undergo photo-induced reduction when exposed to visible light, yielding green solutions from their initial yellow colour. The putative product is a mixed-oxidation (μ-oxo)divanadium (IV/V) species as revealed from EPR, electronic spectroscopy, dynamic ^{1}H NMR, and redox studies.

Keywords. Vanadium; alkali metal; carboxylate analogue; helicate; photo-induced reduction; mixed-valence.

1. Introduction

We have recently examined the coordination chemistry of oxometallate ions with tridentate biprotic dithiocarbazate-based ONS donor Schiff base ligands (H_2L).[1–5] With oxovanadium (IV), the precursor product is a VOL species having one or more available coordination site(s) for the acceptance of ancillary ligands. It has been observed that these coordinatedly unsaturated $LV^{IV}O$ precursors under the mandatory presence of a cationic species, undergo aerial oxidation to anionic *cis*-dioxo LV^VO_2 products.[5] From the close similarity of electronic and molecular structures and coordination behaviour, Floriani *et al.*[6] have proposed that the LVO_2^- unit is an "inorganic analogue" of carboxylate group. The latter is known to coordinate metal ions in a variety of modes (**I–III**) as shown in chart 1. Many interesting clustered and polynuclear metal complexes have been reported recently exploiting these coordination possibilities of carboxylate groups.[7]

In an earlier communication,[5] we have reported the facile aerial oxidation of VOL precursors in the presence of organic base viz. imidazole and its 4-methyl derivative as co-ligands. The products obtained are anionic *cis*-dioxovanadium (V) species stabilized by imidazoleum counter ions, held together by strong hydrogen bonding and Coulombic interactions. Herein we report the coordination behaviour of LVO_2^- (L = L^1 and L^2) moieties towards some alkali metal ions (Na^+ and K^+). Like the carboxylate group, the analogous LVO_2^- ligands have shown interesting diversity in molecular structure in the reported alkali metal adducts (**1**–**3**). Photochemical reactivity of these compounds has been studied in details.

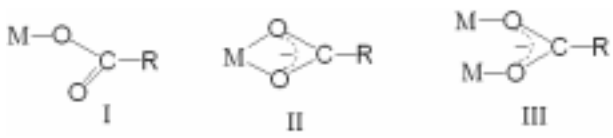

Chart 1.

*For correspondence

2. Experimental

2.1 *Materials*

Ligands H_2L (L = L^1 and L^2) and $[VO(acac)_2]$ were synthesized as described elsewhere.[8,9] Solvents were of reagent grade and were dried from appropriate reagents[10] and distilled under nitrogen prior to their use. All other chemicals were reagent grade, available commercially and used as received.

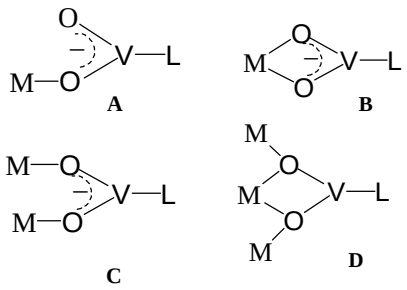

Chart 2.

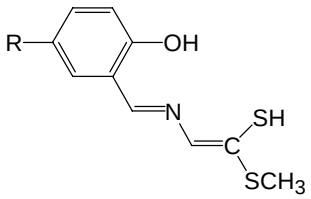

H_2L

X	H_2L
H	H_2L^1
Br	H_2L^2

Table 1. Relevant crystal data for $[L^1VO_2Na(H_2O)_2]_\infty$ (**1**)

Empirical formula	$C_9H_{12}NaN_2O_5S_2V$
fw	366·27
Space group	Monoclinic, $P2_1/c$ (No. 14)
a (Å)	16·005(2)
b (Å)	6·142(1)
c (Å)	14·728(3)
β, deg	101·03(1)
V (Å^3)	1421(1)
Z	4
T (°C)	21 ± 1 °C
λ (MoKα) (Å)	0·71073
ρ_{cacld} (g cm^{-3})	1·71
μ, mm^{-1}	1·04
$R^a(R_w{}^b)$	0·029 (0·085)

$^aR = \sum(||F_o| - |F_c||)/\sum|F_o|$;
$^bR_w = [\sum w(||F_o| - |F_c||)^2/\sum w|F_o|^2]^{1/2}$

2.2 *Physical measurements*

^{1}H NMR spectra were recorded on a Bruker model Avance DPX 300 spectrometer. EPR spectra in the X-band were recorded on a Bruker model ESP 300E spectrometer. Electronic spectra in the near IR region were obtained on a Hitachi U-3400 UV-Vis-NIR spectrometer. Solution electrical conductivity and IR and UV-Vis spectra were obtained as described elsewhere.[11] pH measurements were made with a Systronics model 335 digital pH meter. Cyclic voltammetry in solution was performed with a PAR model 362 scanning potentiostat using Pt working and auxiliary electrodes. A saturated calomel electrode (SCE) was used for reference, and ferrocene, as internal standard.[12] Solutions were ~10^{-3} M in samples and contained 0·1 M TEAP as the supporting electrolyte.

Elemental analyses (for C, H and N) were performed in this laboratory (at IACS) using a Perkin–Elmer 2400 analyser. Sodium contents were estimated using a Thermo Jarrell Ash (model Atom Scan 16) inductively coupled plasma atomic absorption spectrometer.

2.3 *X-ray crystallography*

Diffraction quality crystals of **1** were grown at room temperature by slow evaporation from a methanol–water (1 : 1 *v*/*v*) solution of the compound. A clear yellow elongated plate with dimension 0·40 × 0·30 × 0·05 mm^3 was mounted on a glass fibre and used for data collection at 21 ± 1°C in $\omega - 2\theta$ scan mode on an Enraf–Nonius CAD-4 diffractometer equipped with graphite monochromatized MoK$_\alpha$ (λ = 0·71073 Å) radiation. The background was obtained from an analysis of the scan profile.[13] No crystal decay was observed during the data collection. The unit cell parameters were obtained by least-squares refinement of the angular settings for 25 reflections in the 2θ range 24°–28°.

Crystals of **2** and **3** were grown from solutions of methanol–water (4 : 1 *v*/*v*) and 2-propanol respectively, also by slow evaporation. Intensity data for the yellow fibrous crystals of **2** (0·11 × 0·70 × 0·12 mm^3) and **3** (0·11 × 0·92 × 0·40 mm^3) were collected at room temperature on a Siemens P4 four-circle diffractometer using the $\theta - 2\theta$ technique and graphite monochromatized MoK$_\alpha$ radiation. Relevant crystallographic data for **1** are displayed in table 1 and those for **2** and **3** in table 2.

Table 2. Relevant crystal data for $[(L^2VO_2Na)_2(H_2O)_7]_\infty$ (**2**) and $[L^1VO_2K(H_2O)]_\infty$ (**3**).

	2	**3**
Chem. formula	$Na_2C_{18}H_{28}N_4Br_2S_4O_{13}V_2$	$KC_9H_{10}N_2S_2O_4V$
fw	944·36	364·35
Crystal system	Triclinic	Orthorhombic
Space group	*P*1	*Pbca*
a (Å)	7·739(2)	6·5705(9)
b (Å)	13·810(2)	13·506(2)
c (Å)	16·930(2)	31·332(4)
α (deg)	81·99(8)	90
β (deg)	89·80(13)	90
γ (deg)	76·85(2)	90
V (Å^3)	1744·1(5)	2780·5(7)
Z	2	8
Density, ρ_{cal}, g cm^{-3}	1·798	1·741
T (°C)	20	20
λ (Å)	0·710 73	0·710 73
F (000)	940	1472
abs coeff, mm^{-1}	3·152	1·321
θ range for data collection (deg)	2·43–54·04	3·02–27·49
reflcns collcd	8346	2861
indpdt reflcns (R_{int})	7855 (0·0273)	2861 (0·0000)
*R*1, *wR*2 (all data)	0·0436, 0·0850	0·0288, 0·0777

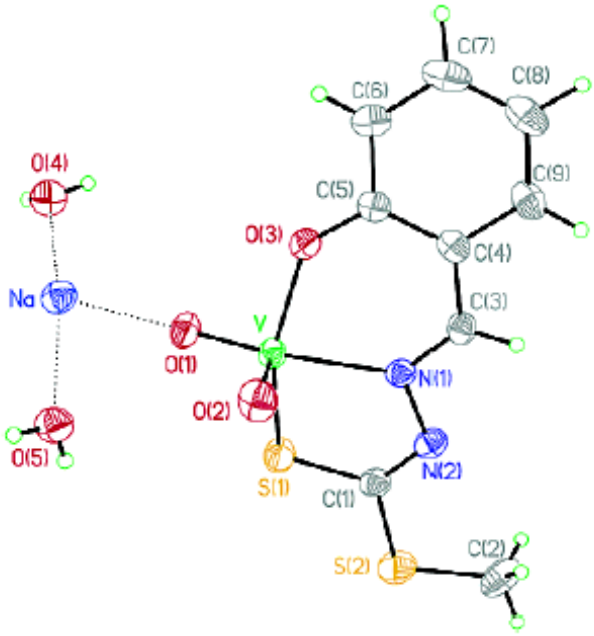

Figure 1. Molecular structure for the complex $[L^1VO_2Na(H_2O)_2]_\infty$ **1** showing the atom numbering (50% probability ellipsoids).

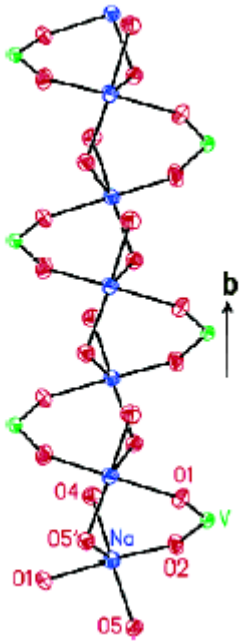

Figure 2. Drawing of the helicate (**1**) viewed parallel to the *b*-axis.

Data for **1** were corrected for Lorentz and polarization effects. An empirical absorption (from 0.762 to 1·000 on *I*) correction was also applied. The maximum 2θ value for data collection was 52·0°. The number of measured reflections was 3184, and of these 2393 unique reflections, which satisfied the $F_0^2 \geq 3{\cdot}0\sigma(F_0^2)$ criterion, were used for structure solution. The structure was solved by direct methods (MULTAN 80)[14] and refined by a full-matrix least-squares procedure minimizing the function $\Sigma\omega(|F_o| -$

Table 3. Selected bond distances and angles for $[L^1VO_2Na(H_2O)_2]_\infty$ (**1**).

Distances (Å)				
V–O(1)	1·648(2)	N(1)–C(3)	1·291(3)	
V–O(2)	1·613(2)	Na–O(1)	2·406(2)	
V–O(3)	1·911(2)	Na–O(2)^b	2·380(2)	
V–S(1)	2·3764(9)	Na–O(4)	2·381(2)	
V–N(1)	2·178(2)	Na–O(5)	2·357(2)	
C(1)–S(1)	1·735(2)	Na–O(5)^b	2·415(2)	
N(1)–N(2)	1·409(2)	Na–S(1)^a	3·177(1)	
Na…Na^b	4·000(2)			
Angles (deg)				
S(1)–V–O(1)	87·85(6)	O(1)–Na–O(5)	93·37(7)	
S(1)–V–O(2)	104·79(7)	O(1)–Na–S(1)^a	84·80(5)	
S(1)–V–O(3)	145·86(5)	O(4)–Na–O(5)^b	87·40(7)	
S(1)–V–N(1)	76·72(5)	O(4)–Na–O(2)^b	100·92(7)	
O(1)–V–O(2)	108·56(8)	O(4)–Na–O(5)	166·40(7)	
O(1)–V–O(3)	96·65(7)	O(4)–Na–S(1)^a	85·47(6)	
O(1)–V–N(1)	150·72(7)	O(5)^b–Na–O(2)^b	83·95(7)	
O(2)–V–O(3)	105·72(8)	O(5)^b–Na–O(5)	106·07(6)	
O(2)–V–N(1)	99·45(8)	O(5)^b–Na–S(1)^a	166·56(6)	
O(3)–V–N(1)	83·49(6)	O(2)^b–Na–O(5)	82·81(7)	
O(1)–Na–O(4)	86·13(7)	O(2)^b–Na–S(1)^a	108·58(5)	
O(1)–Na_O(5)^b	83·37(6)	O(5)–Na–S(1)^a	80·95(5)	
O(1)–Na–O(2)^b	165·19(6)	V–O(1)–Na	125·98(8)	

Hydrogen bond geometry

D–H···A	D···H, Å	H···A, Å	D···A, Å	D–H···Å, deg
O(4)–H(42)···O(1)^c	0·83(3)	2·03(3)	2·827(3)	160(3)
O(5–H(51)···O(4)^d	0·78(3)	2·06(3)	2·812(3)	163(3)
O(5–H(52)···O(3)^e	0·68(4)	2·29(4)	2·937(3)	161(4)

^{a}–*x*, –*y*, –*z*. ^{b}–*x*, *y* + 1/2, –*z* + 1/2. ^{c}–*x*, –*y* + 1, –*z*. ^{d}*x*, *y* – 1, *z*. ^{e}–*x*, *y* – 1/2, –*z* + 1/2

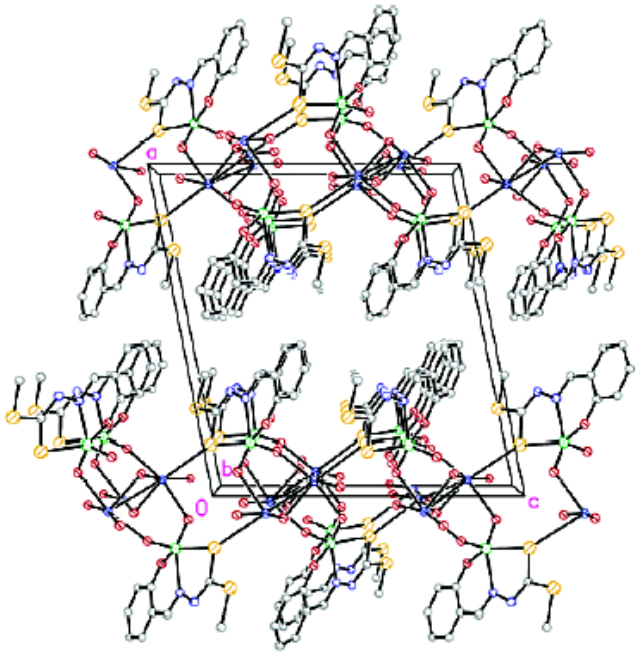

Figure 3. Packing diagram of **1** viewed down the *b* axis showing the linking of the helices into layers.

$|F_c|)^2$, where $\omega = 1/[\sigma^2(F_o^2) + (0{\cdot}0564P)^2 + 0{\cdot}3361P]$ and $P = (F_o^2 + 2F_o^2)/3$. Scattering factors for neutral atoms and the values for $\Delta f'$ and $\Delta f''$ were taken from the usual sources.[15] Non-hydrogen atoms were refined with anisotropic thermal parameters, and hydrogen atoms were included in the model in their calculated positions (C–H, 0·97 Å). The refinements were continued until convergence employing σ weights. Final R and R_w values are 0·029 and 0·085 respectively, and the goodness of fit (S) = 1·108 for 229 refined parameters. The final Fourier difference synthesis showed a maximum and minimum of +0·41(6) and –0·26(6) e/Å^3. Structure refinements were performed by using SHELXL-97.[16] The molecular structures and atom-labelling scheme shown in figures 1–3 were drawn by Bruker SHELXTL package.

Structures of **2** and **3** were also solved by direct methods using SHELXTLPC package.[17] Final refinements were done by a full-matrix least-squares procedure based on all data minimizing $R2 = [\Sigma[w(F_o^2 - F_c^2)^2]/\Sigma(F_c^2)^2]^{1/2}$, $R1 = \Sigma||F_o| - |F_c||/\Sigma|F_o|$,

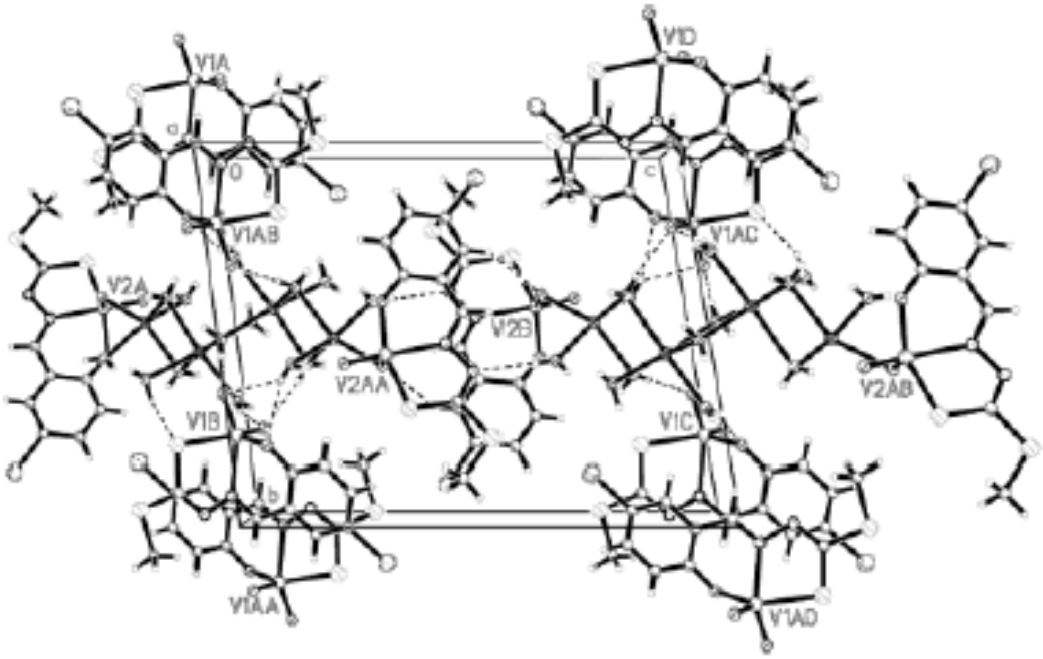

Figure 4. Molecular structure of $[(L^2VO_2Na)_2(H_2O)_7]_\infty$ **2** viewed along the *c* axis.

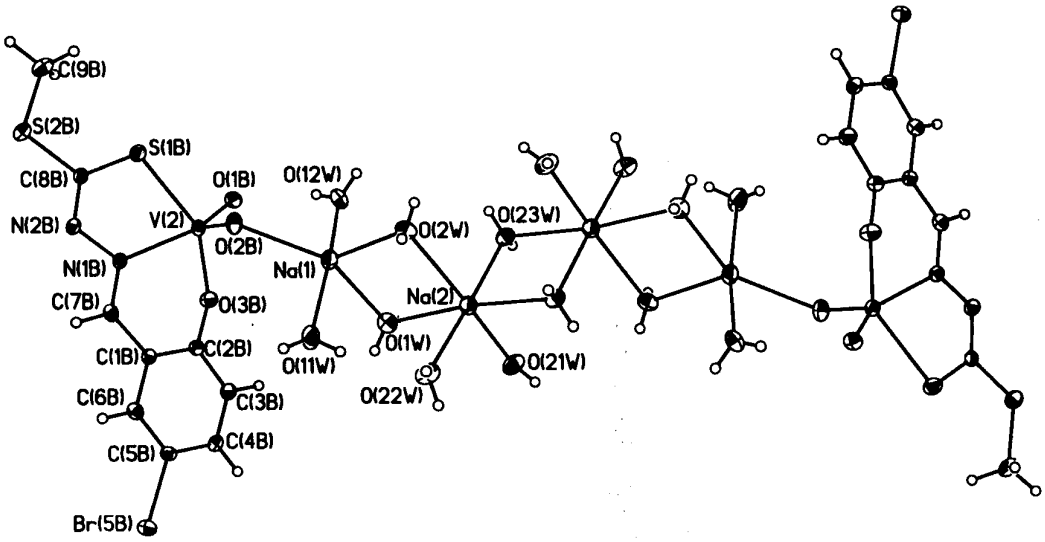

Figure 5. An ORTEP drawing and crystallographic numbering scheme for the cationic part of **2**.

and $S = [\Sigma[w(F_o^2 - F_c^2)^2]/(n-p)]^{1/2}$. All non-hydrogen atoms were refined as anisotropic and the hydrogen atomic positions were fixed relative to the bonded carbon atoms with isotropic parameters fixed.

2.4 *Photochemical studies*

Clear yellow solutions of the complexes (**1**–**3**) in dry acetonitrile were taken in a quartz cell and purged with argon for 20 min. A tungsten filament lamp (60 W) was used as a visible light source to irradiate these solutions which gradually turned green with the passage of time during photolysis. The green solutions obtained after different intervals of exposure time were used for subsequent studies needed for their characterization.

2.5 *Preparation of the complexes*

*$[L^1VO_2Na(H_2O)_2]_\infty$ (**1**)*: To a stirred acetonitrile solution (30 ml) of $[VO(acac)_2]$ (0·4 g, 1·5 mmol) an equimolar amount of the ligand H_2L^1 (0·34 g) in the

Table 4. Selected bond distances (Å) and angles (deg) for $[(L^2VO_2Na)_2(H_2O)_7]_\infty$ (**2**)[a].

Bond lengths			
V(1)–O(2A)	1·620(3)	V(1)–O(1A)	1·652(3)
V(1)–O(3A)	1·914(3)	V(1)–N(1A)	2·167(3)
V(1)–S(1A)	2·3647(14)	V(2)–O(2B)	1·612(3)
V(2)–O(1B)	1·662(3)	V(2)–O(3B)	1·902(3)
V(2)–N(1B)	2·184(3)	N(2)–S(1B)	2·3691(14)
Na(1)–O(11W)	2·284(5)	Na(1)–O(2W)	2·352(4)
Na(1)–O(1W)	2·357(4)	Na(1)–O(12W)	2·387(5)
Na(1)–O(2B)	2·447(3)	Na(2)–O(23W)	2·383(4)
Na(2)–O(22W)	2·400(4)	Na(2)–O(21W)	2·405(5)
Na(2)–O(23W)$^{\#1}$	2·454(4)	Na(2)–O(1W)	2·461(5)
Na(2)–O(2W)	2·516(4)	Na(1)–Na(2)	3·566(3)
Na(2)–Na(2)$^{\#1}$	3·534(4)		
Bond angles			
O(2A)–V(1)–O(1A)	107·8(2)	O(2A)–V(1)–O(3A)	109·3(2)
O(1A)–V(1)–O(3A)	94·61(14)	O(2A)–V(1)–N(1A)	100·21(14)
O(1A)–V(1)–N(1A)	150·9(2)	O(3A)–V(1)–N(1A)	83·01(12)
O(2A)–V(1)–S(1A)	107·37(12)	O(1A)–V(1)–S(1A)	87·28(12)
O(3A)–V(1)–S(1A)	140·64(10)	N(1A)–V(1)–S(1A)	77·00(9)
O(2B)–V(2)–O(1B)	107·7(2)	O(2B)–V(2)–O(3B)	105·1(2)
O(1B)–V(2)–O(3B)	96·28(14)	O(2B)–V(2)–N(1B)	100·24(14)
O(1B)–V(2)–N(1B)	151·0(2)	O(3B)–V(2)–N(1B)	83·43(13)
O(2B)–V(2)–S(1B)	107·85(13)	O(1B)–V(2)–S(1B)	87·29(11)
O(3B)–V(2)–S(1B)	144·01(11)	N(1B)–V(2)–S(1B)	76·86(10)
O(11W)–Na(1)–O(2W)	94·9(2)	O(11W)–Na(1)–O(1W)	79·7(2)
O(2W)–Na(1)–O(12W)	98·3(2)	O(1W)–Na(1)–O(12W)	92·2(2)
O(11W)–Na(1)–O(2B)	93·8(2)	O(2W)–Na(1)–O(2B)	125·6(2)
O(1W)–Na(1)–O(2B)	146·6(2)	O(2W)–Na(1)–O(1W)	87·8(2)
O(11W)–Na(1)–O(12W)	164·2(2)	O(12W)–Na(1)–O(2B)	85·4(2)
O(23W)–Na(2)–O(22W)	176·2(2)	O(23W)–Na(2)–O(21W)	83·5(2)
O(22W)–Na(2)–O(21W)	100·1(2)	O(22W)–Na(2)–O(23W)$^{\#1}$	97·7(2)
O(21W)–Na(2)–O(23W)$^{\#1}$	89·4(2)	O(23W)–Na(2)–O(1W)	97·7(2)
O(22W)–Na(2)–O(1W)	83·8(2)	O(21W)–Na(2)–O(1W)	86·0(2)
O(23W)$^{\#1}$–Na(2)–O(1W)	173·6(2)	O(23W)–Na(2)–O(2W)	87·1(2)
O(22W)–Na(2)–O(2W)	89·7(2)	O(21W)–Na(2)–O(2W)	163·6(2)
O(23W)$^{\#1}$–Na(2)–O(2W)	103·4(2)	O(1W)–Na(2)–O(2W)	82·01(4)

[a]Symmetry transformations used to generate equivalent atoms: (#1) $-x + 4, -y - 1, -z + 2$

same solvent (15 ml), was added and the mixture was refluxed for 10 min to get a clear brown solution. To this was then added an aqueous solution (5 ml) of sodium carbonate (0·10 g), and the resulting solution was further refluxed for 1 h. The green solution obtained at this stage was filtered and the filtrate allowed to stand in the air for several days becoming gradually yellow in colour. The solution was rotary evaporated to about 15 ml in volume when a yellow crystalline product slowly began to appear. It was collected by filtration, washed with methanol/Et_2O (1 : 1 *v*/*v*), and finally dried *in vacuo*. The product was recrystallized from methanol. Yield: 0·34 g (62%). Anal. Calcd for $C_9H_{12}NaN_2O_5S_2V$: C, 29·51; H, 3·28; N, 7·65; Na, 6·28%. Found: C, 29·90; H, 3·29; N, 7·80; Na, 6·32%. IR (KBr disk, cm^{-1}): ν(OH), 3480, 3380 (b); ν(C=N), 1600(s); ν(C–O/phenolate), 1540(s); $\nu(V{=}O_t)$, 970, 900(s). UV-Vis (CH_3OH) [λ_{max}, nm (ε, M^{-1} cm^{-1})]: 393 (8200), 290 (26100), 230 (31500).

*$[(L^2VO_2Na)_2(H_2O)_7]_\infty$ (**2**)*: An analogous method of preparation as described above for **1** was employed using the bromo derivative of the ligand (H_2L^2). Drying under vacuum was avoided due to impending loss of water of crystallization. Yield: 56%. Anal. Calcd for $C_{18}H_{28}Br_2Na_2N_4O_{13}S_4V_2$: C, 22·88; H, 2·97; N, 5·93%. Found: C, 23·20; H, 2·90; N, 6·0%. IR (KBr disk, cm^{-1}): ν(OH), 3400(b); ν(C=N), 1596(s); ν(C–O/phenolate), 1535(s); $\nu(V{=}O_t)$, 948, 900(s).

Table 5. Selected bond distances (Å) and angles (deg) for $[L^1VO_2K(H_2O)]_\infty$ (**3**)[a].

Bond lengths (Å)			
V–O(3)	1·622(2)	V–O(2)	1·651(2)
V–O(1)	1·924(2)	V–N(3)	2·180(2)
V–S(1)	2·3846(8)	K–O(3)$^{\#1}$	2·714(2)
K–O(1W)	2·800(3)	K–O(1)$^{\#2}$	2·824(2)
K–O(2)	2·874(2)	K–O(1W)$^{\#1}$	2·894(3)
K–O(2)$^{\#2}$	2·895(2)	K–O(3)	2·974(2)
O(3)–K$^{\#2}$	2·714(2)	O(2)–K$^{\#1}$	2·895(2)
O(1)–K$^{\#1}$	2·824(2)	O(1W)–K$^{\#2}$	2·894(3)
K–K$^{\#1}$	3·7921(8)	K–K$^{\#2}$	3·7921(8)
Bond angles (deg)			
O(3)–V–O(2)	107·07(10)	O(1)–V–O(3)	106·95(9)
O(2)–V–O(1)	95·09(9)	O(3)–V–N(1)	102·97(9)
O(2)–V–N(1)	149·00(9)	O(1)–V–N(1)	83·22(7)
O(3)–V–S(1)	101·37(7)	O(2)–V–S(1)	89·68(7)
O(1)–V–S(1)	148·40(6)	N(1)–V–S(1)	76·95(5)
O(3)–V–K	55·23(8)	O(2)–V–K	51·84(7)
O(1)–V–K	108·38(5)	N(1)–V–K	157·12(6)
O(1W)–K–O(2)	128·59(7)	O(3)$^{\#1}$–K–O(1W)$^{\#1}$	77·92(8)

Hydrogen bonding parameters (Å, deg)				
D–H···A	*d*(D···H)	*d*(H···A)	*d*(D···A)	∠DHA
O(1W)–H(2W)···O(2)$^{\#3}$	0·82(6)	2·40(6)	3·156(3)	154(5)
O(1W)–H(1W)···O(3)$^{\#2}$	0·72(7)	2·55(6)	3·047(4)	128(6)
O(1W)–H(1W)···S(2)$^{\#4}$	0·72(7)	2·99(6)	3·620(3)	147(6)

[a]Symmetry transformations used to generate equivalent atoms: (#1)$x + 1/2, y, -z + 1/2$; (#2) $x - 1/2, y, -z + 1/2$; (#3) $-x, y - 1/2, -z + 1/2$; (#4) $-x - 1, y - 1/2, -z + 1/2$

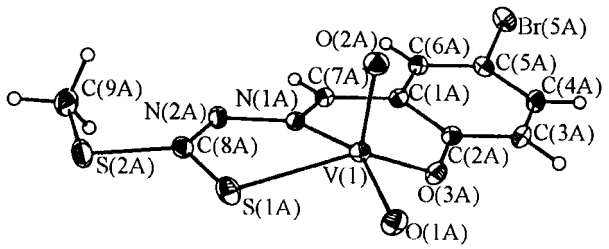

Figure 6. An ORTEP drawing and crystallographic numbering scheme for the anionic part of **2**.

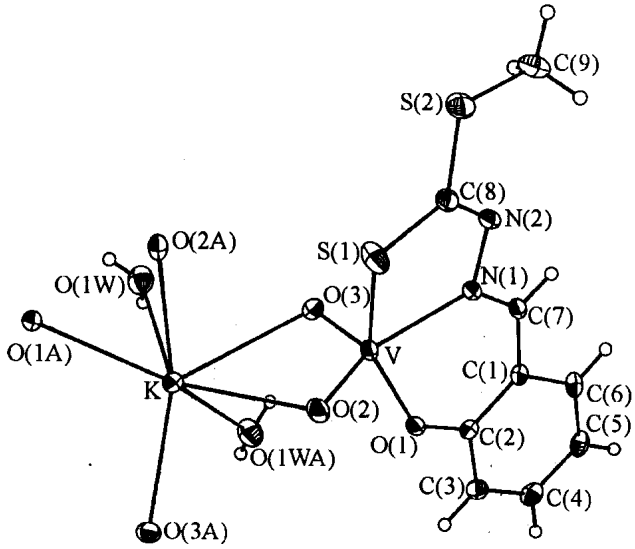

Figure 7. Molecular structure of the monomeric unit of $[L^1VO_2K(H_2O)]_\infty$ **3**, showing the atom-labelling scheme.

$[L^1VO_2K(H_2O)]_\infty$ (3): To a solution of $[VO(acac)_2]$ (0·26 g, 1 mmol) in acetonitrile (10 ml) was added, under stirring, a solution of H_2L^1 (0·23 g, 1 mmol), also dissolved in the same solvent (20 ml). The solution was refluxed for 10 min, combined with an aqueous solution (5 ml) of potassium carbonate (0·17 g), and refluxed further for 1 h to give a green solution. It was filtered and the filtrate allowed to stand in the air for several days becoming gradually yellow in colour. The yellow solution was rotary-evaporated to near dryness, extracted with 2-propanol (15 ml), and filtered. The filtrate was cooled to 4°C for an overnight period to give a yellow crystalline product. It was collected by filtration, washed with Et_2O (4×10 ml), and dried in the air. The product was

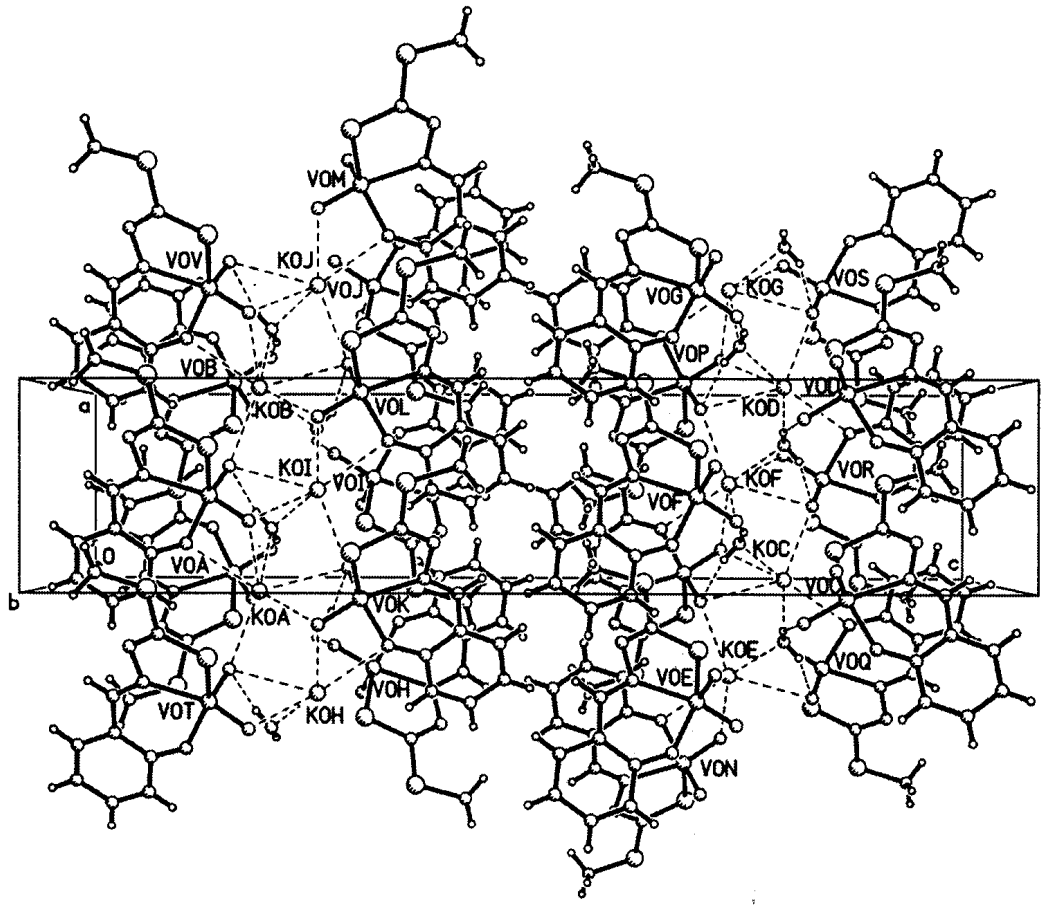

Figure 8. Hydrogen-bonded extended-chain structure of **3**, viewed along the *a* axis.

recrystallized from 2-propanol. Yield: 0·19 g (53%). Anal. Calcd for $C_9H_{10}KN_2O_4S_2V$: C, 29·67; H, 2·75; N, 7·69%. Found: C, 28·90; H, 2·70; N, 7·40%. IR (KBr disk, cm^{-1}): ν(OH), 3470(b); ν(C=N), 1604(s); ν(C–O/phenolate), 1545(s); ν(V=O_t), 936, 888(s).

3. Results and discussion

3.1 *Syntheses*

Complexes **1**–**3** were prepared by the reaction of $[VO(acac)_2]$ with the tridentate ONS ligands (H_2L^1 and H_2L^2) in CH_3CN/water medium in the presence of alkali metal carbonate. Obligatory steps in this preparative procedure are the presence of water in the reaction medium and its subsequent exposure to atmospheric oxygen as confirmed by several control experiments. The reaction usually proceeds through a green vanadium (IV) intermediate which subsequently undergoes aerial oxidation to yellow anionic *cis*-dioxovanadium (V) species. The carbonate anion possibly plays a crucial role in this oxidation process as no other common alkali metal salts are found to be as effective to carry out such reaction. The products **1**–**3** have infinite chain structures in the solid state with interesting variations as confirmed by X-ray crystallography (see below), involving anionic LVO_2^- units coordinated like an analogue of carboxylate group to aquated alkali metal ions. The cationic and anionic parts in these compounds are held together by the process of self-assembly[18] through the simultaneous use of Coulombic interactions and efficient hydrogen bonding. Interestingly, the structure of **1** offers a rare example of a single-stranded helix (see below) with sodium ions forming the axis.[19] The bent LVO_2^- unit with a formal negative charge on it binds the aquated sodium ion in a *bis*-monodentate manner to generate the infinite helical strand.

IR spectra of the complexes have all the characteristic bands of the coordinated tridentate ligands.[2] In addition, the compounds exhibit a strong two-band pattern, appearing in the 970–888 cm^{-1} region

due to V=O_t terminal stretches, typical of the *cis*-VO_2 core.[20] Broad medium intensity band(s) in the high-frequency region 3480–3380 cm^{-1} indicates the presence of coordinated water in these compounds.

3.2 *Description of crystal structures*

The molecular structure of **1** is shown in figure 1. Important inter atomic parameters are listed in table 3. The molecule when viewed along the *b*-axis, exhibits an infinite spiral of an ⋯ O ⋯ V ⋯ O ⋯ Na ⋯ O ⋯ chain as shown in figure 2. Individual vanadium (V) centres exist in a distorted square pyramidal geometry (figure 1), with the four basal positions from the tridentate ligand and one of the terminal oxo ligands O(1) of the *cis*-VO_2 core. The axial site is occupied by the remaining oxo ligand O(2) which forms angles in the range 99·45(8)–108·56(8)° with the basal plane. The angles O(3)–V–S(1) and O(1)–V–N(1) are 145·86(5) and 150·72(7)°, respectively which indicate that the central vanadium atom is shifted slightly (0·5097(8) Å) out of the basal plane towards the apical oxygen O(2) atom. The O(1)–V–O(2) angle (108·56(8)°) and the terminal V=O distances (1·648(2) and 1·613(2) Å) are in the expected range.[20]

An intriguing structural feature of this compound is the presence of hexacoordinated sodium ion centres, each acting as a bridge between the two neighbouring LVO_2 moieties. As shown in figure 2, each LVO_2 moiety in turn is bound to two adjacent sodium ions through terminal oxo ligands, thus forming an infinite helicate with a single strand of alternating Na ions and LVO_2 moieties, and there are two of these units in each turn (along the 2_1 axis). The Na⋯Na distance between the immediate neighbours is 4·000(2) Å. Besides the terminal oxo ligands, each sodium ion also has two types of water molecule in its coordination sphere. One is exclusively attached to a single sodium ion as denoted by O(4) and the other, denoted by O(5), occupies a bridging position between the two adjacent sodium ions. Thus, two vanadyl oxo atoms O(2) and O(1)′ from two different vanadyl centres and an oxygen atom O(5)′ from a bridging water molecule constitute three atoms of the equatorial plane, while the apical sites are occupied by O(4) and O(5) oxygen atoms (O(4)–Na–O(5), 166.40(7)°) of a non-bridging and bridging water molecule. The sixth coordination site is occupied by S(1) from a neighbouring helicate strand, thus linking the helicates into a layer perpendicular to *a*. In this manner, the structure may be described as hydrophilic layers separated by hydrophobic layers due to the organic moieties (figure 3). There are several secondary interactions in this molecule, viz. between O(1)–O(4), O(5)–O(3) and O(5)–O(4) atoms, all through strong hydrogen bonds as listed in table 3. These hydrogen-bonding interactions play a major role in stabilizing this unusual helical structure. Very few helicate molecules[21-23] are known in which hydrogen bonding exerts such a delicate influence as is observed in biological helices.

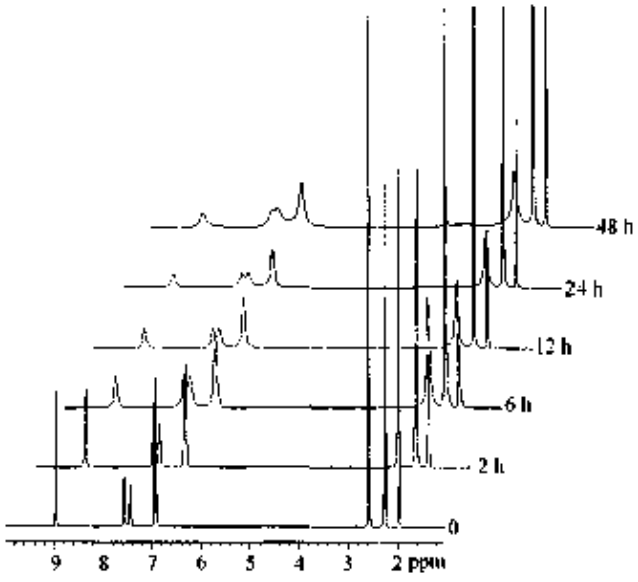

Figure 9. Time-dependent ^{1}H NMR spectra of **1** in acetonitrile-d_3 solution under the exposure of visible light, showing gradual line broadening.

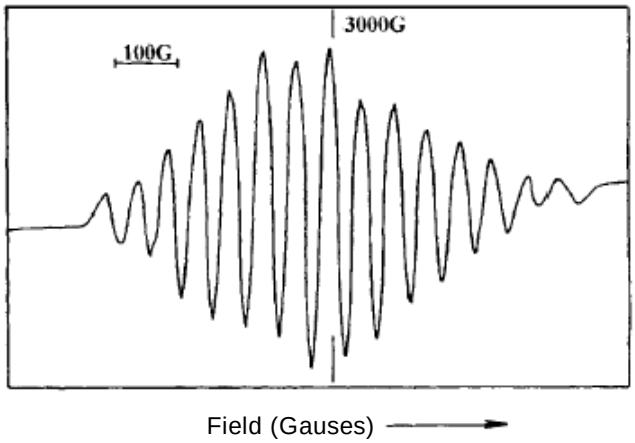

Figure 10. X-band EPR spectrum of a photo-reduced solution of **1** in acetonitrile at room temperature.

Molecular structure of **2** reveals a hydrogen-bonded infinite assembly of stoichiometry $[(L^2VO_2Na_2(H_2O)_7)_2(L^2VO_2)_2]_\infty$ (figure 4). The molecule contains a cationic (figure 5) and an anionic part (figure 6), both involving L^2VO_2 units which are structurally nonequivalent. Relevant metrical parameters are summarized in table 4. Vanadium centres in both the parts have distorted square-pyramidal geometry with donor atoms (S, N and O) from the tridentate ligand and one of the terminal oxo atoms O(1B) [O(1A) for the anionic part] of the *cis*-VO_2 core forming the basal plane. The apical position is occupied by the remaining oxo ligand O(2B) [O(2A)] which forms angles in the range 100·24(14)–107·85(13)° [100·21(14)–109.3(2)°] with the basal plane. The terminal V=O_t distances 1·612(3) and 1·662(3) Å [1·620(3) and 1·652(3) Å] and O(1)–V–O(2) angle 107·7(2)° [107·8(2)°] are in the expected range for a *cis*-VO_2^+ core.[20]

The cationic part of the complex is centrosymmetric (figure 5) involving two L^2VO_2 units connected by a zigzag chain comprising four aquated sodium ion centres. The terminal sodium ion Na(1) has trigonal bipyramidal geometry with the equatorial positions occupied by O(1W) and O(2W) from the two bridging aqua ligands in addition to a terminal oxo ligand O(2B) [Na(1)–O(2B), 2·447(3) Å] of a L^2VO_2 core. The axial positions are occupied by two more aqua ligands O(11W) and O(12W) of non-bridging type. The distances of Na(1) from O(1W), O(2W) and O(12W) are almost identical [in the range 2·352(4)–2·387(5) Å], while the remaining aqua ligand O(11W) is closer [Na(1)–O(11W), 2·284(5) Å] to the metal centre. The sum of the three basal angles at sodium is 360° and the Na(1) atom is displaced by 0·0323 Å from this least-squares basal plane towards the apical O(11W) atom.

Na(1) is connected to the central octahedral sodium ion Na(2) by the bridging oxygen atoms O(1W) and O(2W), the distances being Na(1)…Na(2) 3·566(3) Å, Na(2)–O(1W) 2·461(5) Å and Na(2)–O(2W) 2·516(4) Å. The remaining coordination sites of Na(2) are occupied by two bridging O(23W), O(23W) # 1 and two non-bridging O(21W) and O(22W) aqua ligands with distances (Na–O(W)) in the range 2·383(4)–2·454(4) Å. The former two oxo ligands are used to bind Na(2) with an identical atom Na(2) # 1 of the other half of this centrosymmetric ion (figure 5), the Na(2)…Na(2) # 1 separation being 3·534(4) Å. Each cationic part, for charge counter balance requires two anionic parts which remain interlocked by strong hydrogen bonding (figure 4).

Crystallographic analysis of $[L^1VO_2K(H_2O)]_\infty$ **3** reveals an extended hydrogen bonded structure as well. A perspective view of the monomeric unit is shown in figure 7 and the relevant bonding parameters in table 5. The molecule when viewed along the *a* axis, exhibits an infinite array of alternating $L^1VO_2^-$ and aquated K^+ ions, held together by strong hydrogen bonding and Coulombic interactions (figure 8). Individual vanadium (V) centres exist in a distorted square pyramidal geometry, as in **1**, with the basal positions being occupied by the donor atoms from the tridentate ligand together with a terminal oxo group O(2). The apical position is occupied by the remaining oxo atom O(3). The metrical parameters are similar to those in **1**. The L^1VO_2 unit is bound to the K^+ ion by both the terminal oxo atoms, the distances K–O(2) and K–O(3) are 2·874(2) and 2·974(2) Å respectively.

An interesting aspect of this structure is the presence of seven-coordinated K^+ ion centres each acting as a bridge among three neighbouring $L^1VO_2^-$ moieties (figure 7). Besides O(2) and O(3) as described above, the remaining five coordination sites around K are occupied by the oxo groups O(2A) and O(3A), each belongs to a different but adjacent $L^1VO_2^-$ unit, phenoxo oxygen O(1A) and two bridging aqua ligands O(1W) and O(1WA) that help in the propagation of chain (figure 8). All these K–O bonds have nearly identical lengths which fall in the range 2·714(2)–2·895(2) Å. In the process, the $L^1VO_2^-$ units here show a very interesting bonding behaviour. While it binds a central K^+ ion in a chelated fashion (mode II) as mentioned above (in chart 1), it also bridges (mode D in chart 2) two adjacent K^+ ions (K #1 and K #2) at the same time [O(2)–K #1, 2·895(2) and O(3)–K #2, 2·714(2) Å]. The distances K…K #1 and K…K #2 are identical 3·7921(8) Å. There are several secondary interactions in this molecule, viz. between O(1W)–O(2), O(1W)–O(3) and O(1W)–S(2), all through strong hydrogen bonds as listed in table 5. These hydrogen bonding interactions play a crucial role in stabilizing this extended structure with potassium ions forming an ion channel (figure 8).

3.3 *Structure in solution*

Solutions of **1**–**3** in water and methanol are stable for several days and show feeble electrical conductivities (Λ_M in water, 20–35 Ω^{-1} cm^2 mol^{-1}), giving clear indication that the alkali metal ions remaining

Table 6. Comparison between the physical characteristics, spectroscopic and electrochemical features of compound **4** and the photo-reduced product **1a**.

Characteristics	Compound **4**	Photo-reduced product **1a**
Solution colour	Green	Green
EPR features at room temperature	15-line $\langle g \rangle = 2{\cdot}128$ $\langle A \rangle \times 10^4 = 44\ cm^{-1}$	15-line $\langle g \rangle = 2{\cdot}136$ $\langle A \rangle \times 10^4 = 48{\cdot}4\ cm^{-1}$
Intervalence transfer (IT) band in CH_3CN	970 nm	970 nm
Cyclic voltammetric feature ($E_{1/2}$ vs SCE) in CH_3CN	0·42 V	0·44 V

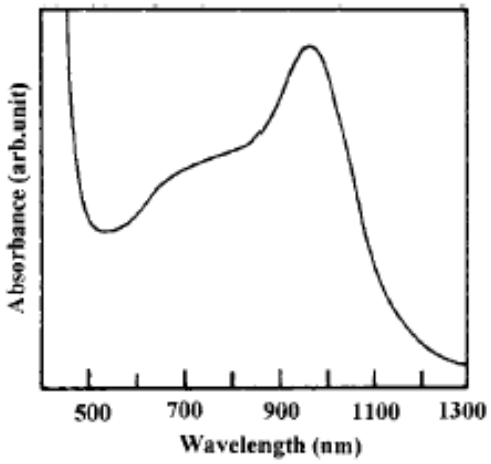

Figure 11. VIS–NIR electronic absorption spectrum of a photo-reduced solution of **1** ($\approx 1{\cdot}0 \times 10^{-3}$ M) in acetonitrile after 12 h exposure to visible light.

coordinated in solution as in the solid state. In dry aprotic solvents viz. acetonitrile, DMF or DMSO, fresh yellow solutions of these compounds gradually turn green with the exposure to visible light. Progress of the photochemical reaction in CH_3CN was followed by ^1H NMR experiments. The results are displayed in figure 9 for a representative compound **1** which reveals gradual loss of resolution as well as line-broadening of the main spectral features with increase in exposure time. The results indicate generation of a paramagnetic species by reduction through a photochemical pathway as confirmed by control experiments.

3.4 *Identification of the photo-reduced product*

In spite of our best effort, we were unable to isolate the green paramagnetic photo-reduced products **1a**–**3a** (corresponding precursor complexes being **1**–**3**, respectively) in the solid state. These green paramagnetic products, unlike their precursors, are EPR active, providing a fifteen-line spectrum at room temperature (as shown in figure 10 for a representative product **1a**) with $\langle g \rangle = 2{\cdot}136$. This indicates generation of a species involving a coupled vanadium ($I = 7/2$) centre with an odd interacting electron. The hyperfine splitting parameter $\langle A \rangle_{15}$, $48{\cdot}4 \times 10^{-4}$ cm^{-1} in this case is almost half of that of a localized spectrum ($\langle A \rangle_8$, 89×10^{-4} cm^{-1}) reported earlier[3] for a μ-oxo divanadium (IV/V) compound with closely similar ligands. This observation again speaks in favour of **1a** to be a dinuclear species[24] with mutually interacting vanadium (IV/V) centres.

As mentioned in the experimental section, a freshly prepared solution of **1** in acetonitrile is optically transparent in the near IR–Vis region. The green photo-reduced solution however absorbs in the 1300–500 nm range, generating a broad well-developed band of moderately high intensity at 970 nm along with a low intensity shoulder centred at 710 nm, A_{970}/A_{710} being close to 1·60 after a 12 h exposure time (figure 11). While the near-IR band (at 970 nm), on the basis of its shape and intensity, is anticipated as arising from an intervalence transfer (IT) transition, the absorption in the visible region (at 710 nm) is more likely to have a ligand–field origin localized on an oxovanadium (IV) centre.[2]

Recently we have been successful in synthesizing mixed–oxidation divanadium (IV/V) compounds[2,3] containing a $V_2O_3^{3+}$ core with the same and related ligands. One of these compounds (BzImH) [L^IOV^{IV}–O–V^VOL^I] (BzIm = benzimidazole), **4** with the same ONS donor ligand as in **1**, has been structurally characterized.[2] Some of the relevant physicochemical data for **4** are displayed in table 6 along with those of compound **1a** for a direct comparison. The observed similarities strongly suggest the generation of a mixed-oxidation divanadium(IV/V) compound during photo–induced reduction of **1** in dry aprotic solvents. Almost similar results are obtained with **2** and **3** under identical reaction conditions.

Conclusions

Attempts have been made in recent times to compare certain oxo-vanadium species as 'inorganic analogues of organic functionalities' because of some structural and chemical properties they have in common.[6] The role of LVO_2^- species here is a case in point where the *cis*-dioxovanadium (V) moiety behaves like an analogue of a carboxylate group, holding the adjacent alkali metal ions together through various binding patterns (chart 2). For example, with sodium ion in **2**, the mode of binding is simple monodented (**A**) while in **1** an interesting *bis*-monodented type (**C**) of attachment is observed. With potassium however, the binding pattern in **3** is much more complicated involving both **B** and **D** types of attachment. Compound **1** is a rare example of an 'inorganic helix' where hydrogen bonding plays a central role in stabilizing a single-stranded structure with labile sodium ion centres occupying the axis.

In aprotic solvents of higher donor capacity, these extended hydrogen-bonded structures collapse when the compounds are irradiated with visible light. The putative product, formed due to photo-induced reduction, is a mixed-oxidation coupled divanadium (IV/V) species with a delocalized electronic structure on the time-scale of EPR spectroscopy.

Acknowledgements

We are grateful to the Council of Scientific and Industrial Research, New Delhi for financial support. We thank Professor A Alan Pinkerton (University of Toledo) and Professor Ray J Butcher (Howard University) for their help in crystal structure analyses.

References

1. Dutta S K, McConville D B, Youngs W J and Chaudhury M 1997 *Inorg. Chem.* **36** 2517
2. Dutta S K, Kumar S B, Bhattacharyya S, Tiekink E R T and Chaudhury M 1997 *Inorg. Chem.* **36** 4954
3. Dutta S K, Samanta S, Kumar S B, Han O H, Burckel P, Pinkerton A A and Chaudhury M 1999 *Inorg. Chem.* **38** 1982
4. Dutta S K, Samanta S, Ghosh D, Butcher R J and Chaudhury M 2002 *Inorg. Chem.* **41** 5555
5. Samanta S, Ghosh D, Mukhopadhyay S, Endo A, Weakley T J R and Chaudhury M 2003 *Inorg. Chem.* **42** 1508
6. Giacomelli A, Floriani C, De Souza Duarte A O, Chiesi-Villa A and Guastini C 1982 *Inorg. Chem.* **21** 3310
7. See for example: (a) Chang A, Francesconi L C, Malley M F, Kumar K, Gougoutas J Z, Tweedle M F, Lee D W and Wilson L J 1993 *Inorg. Chem.* **32** 3501; (b) Yukawa Y, Igarishi S, Yamano A and Sato S 1997 *Chem. Commun.* 711; (c) Harben S M, Smith P D, Beddoes R L, Collison D and Garner C D 1997 *Angew. Chem., Int. Ed. Engl.* **36** 1897; (d) Powell A K, Heath S L, Gatteschi D, Pardi L, Sessoli R, Spina G, Del Giallo F and Pieralli F 1995 *J. Am. Chem. Soc.* **117** 2491; (e) Smith P D, Berry R E, Harben S M, Beddoes R L, Helliwell M, Collison D and Garner C D 1997 *J. Chem. Soc., Dalton Trans.* 4509
8. Dutta S K, Tiekink E R T and Chaudhury M 1997 *Polyhedron* **16** 1863
9. Rowe R A and Jones M M 1957 *Inorg. Synth.* **5** 113
10. Perrin D D, Armarego W L F and Perrin D R 1980 *Purification of laboratory chemicals* 2nd edn (Oxford, England: Pergamon)
11. (a) Dutta S K, McConville D B, Youngs W J and Chaudhury M 1997 *Inorg. Chem.* **36** 2517; (b) Bhattacharyya S, Weakley T J R and Chaudhury M 1999 *Inorg. Chem.* **38** 633
12. Gagné R R, Koval C A and Lisensky G C 1980 *Inorg. Chem.* **19** 2854
13. Blessing R H, Coppens P and Becker P 1974 *J. Appl. Crystallogr.* **7** 488
14. Main P, Fiske S J, Hull S E, Germain G, Declerq J P and Wollfson N M 1980 MULTAN 80, University of York, England
15. International tables for X-ray crystallography 1974 (Birmingham: Kynoch Press) vol. 4 (Present distributor – Dordrecht: Kluwer Academic Publishers)
16. Sheldrick G M 1997 SHELXL-97 University of Göttingen: Göttingen, Germany
17. Sheldrick G M 1996 SHELXLTLPC and SHELXTL, Program for Crystal Structure Determination; Cambridge University: Cambridge, England
18. Philip D and Stoddart J F 1996 *Angew. Chem., Int. Ed. Engl.* **35** 1154
19. Bell T W and Jousselin H 1994 *Nature* (*London*) **367** 441
20. Li X, Lah M S and Pecoraro V L 1988 *Inorg. Chem.* **27** 4657
21. Ezuhara T, Endo K and Aoyma Y 1999 *J. Am. Chem. Soc.* **121** 3279
22. Batten S R, Hoskins B F and Robson R 1997 *Angew. Chem., Int. Ed. Engl.* **36** 636
23. Libman J, Tor Y and Shanzer A 1987 *J. Am. Chem. Soc.* **109** 5880
24. Slichter C P 1955 *Phys. Rev.* **99** 478